Analytical Chemistry Research 4 (2015) 1–7

Contents lists available at ScienceDirect

Analytical Chemistry Research

journal homepage: www.elsevier.com/locate/ancr

Towards broadening thermospray flame furnace atomic absorption spectrometry: Influence of organic solvents on the analytical signal of magnesium

Ezequiel Morzan [a], Jorge Stripeikis [a,b], Mabel Tudino [a,*]

[a] Laboratorio de Análisis de Trazas. INQUIMAE, Departamento de Química Inorgánica, Analítica y Química Física, Universidad de Buenos Aires, Pabellón 2, Ciudad Universitaria, (1428) Buenos Aires, Argentina
[b] Departamento de Ingeniería Química, Instituto Tecnológico de Buenos Aires, Av Eduardo Madero 399 C1106, Buenos Aires, Argentina

ARTICLE INFO

Article history:
Received 15 December 2014
Revised 18 February 2015
Accepted 19 February 2015
Available online 5 March 2015

Keywords:
Thermospray
Organic solvents
Droplet size
Cell temperature
Optimization of the analytical signal
Magnesium determination

ABSTRACT

This study demonstrates the influence of the solvent when thermospray flame furnace atomic absorption spectrometry (TS-FF-AAS) is employed for the determination of elements of low volatility, taking magnesium (Mg) as leading case. Several organic solvents/water solutions of different characteristics (density, surface tension, viscosity, etc.) and proportions were employed for the TS-FF-AAS analytical determination. To this end, solutions containing methanol, ethanol and isopropanol in water were assayed. Measurements were performed at different acetylene/air ratios of the combustion flame and then, the corresponding response surfaces were obtained. Methanol/water 75% v/v as carrier and a fuel rich flame were found as the most sensitive alternative.

In the light of these findings and in order to explain the changes on the analytical signal, the influence of the solvent characteristics, the sample droplet size and the redox environment was studied. An estimation of the temperature of different zones of the heated flame furnace based on a modified signal ratio pyrometry method was analyzed for comparative purposes. A full discussion is provided throughout the paper.

Once obtained the best conditions for analysis, Mg was determined in samples of effervescent vitamin tablets comparing two different solvents. The tablets were dissolved in methanol/water 75% v/v and ethanol/water 75% v/v and then, directly introduced in the TS device. The methanol/water 75% v/v dissolution yielded a slightly higher sensitivity when compared to ethanol/water and thus, the latter was selected due to its lower toxicity. The obtained figures of merit are: LOD (3σb): 0.021 mg L^{-1}; LOQ (10σb): 0.068 mg L^{-1}, sensitivity: 0.086 L mg^{-1}; RSD%: 3.55, dynamic linear range 0.068–5 mg L^{-1}. Comparison of the results was performed by flame atomic absorption spectrometry (FAAS), showing a good agreement (95% confidence level, $n = 5$). Whilst the FAAS approach needed sample mineralization as no complete solubility was attained with both alcohol/water solvents, TS allowed direct introduction of the sample with an excellent recovery of the analyte after spiking. The whole TS procedure was more economic (lower amount of reagents and wastings, lower time of operation) and faster (60 h^{-1} sampling throughput) than FAAS.

Nonetheless, the main objective of this work is to show that an analytical signal different from zero can be obtained for Mg via TS by simply choosing the adequate operational variables that allow an optimization of the mass transfer of the analyte into the atomizer and a favorable dynamics of desolvation/atomization.

This approach could broad TS analytical capabilities to other elements of lower volatility as it is shown here for the case of Mg.

1. Introduction

Thermospray flame furnace atomic absorption spectrometry (TS-FF-AAS) is a method of analysis proposed by Gaspar and Berndt [1] where a liquid sample is transported through a ceramic

* Corresponding author. Tel.: +54 1145763360; fax: +54 1145763341.
E-mail address: tudino@qi.fcen.uba.ar (M. Tudino).

http://dx.doi.org/10.1016/j.ancr.2015.02.002
2214-1812/

capillary towards a perforated metallic tube (mostly nickel) located over a combustion flame in the optical path of an atomic absorption spectrometer. This arrangement allows the complete sample introduction and an increased residence time of the analyte in the furnace, improving sensitivities for the volatile elements (Cd, Zn and Pb) [2–10]. Nonetheless, a drawback of this technique is that a fraction of the flame energy is wasted on solvent vaporization producing a cooler environment in the atomization cell. This is why most of the literature in thermospray (TS) reports the analytical determination of elements of low atomization temperatures or derivatization strategies for the less volatile ones [11–16].

Since the early works of Berndt et al. up to date, no Mg determination by TS-FF-AAS was reported due to the lack of sensitivity [13,15]. This is probably because the environment inside the perforated atomization cell and its lower temperature -when compared to the premixed air/acetylene flame-, produce a decrease in the atomic population.

This work seeks for the first time alternatives to control the cooling of the atomization cell, providing at the same time a suitable redox environment able to minimize the amount of oxygen and thus, the amount of oxygenated compounds that magnesium is prone to produce. In this way, the addition of organic compounds seemed to be capable of consuming oxygen by combustion. At the same time, the reduction of the droplet size should enable a more favorable desolvation/atomization dynamics.

Even though this is not the first time that organic compounds are employed as carriers in TS, the literature [16–18], mostly refer to applications of sample introduction into mass spectrometers where the reduction of the droplet size becomes an important advantage. Few approaches for elemental determination were reported up to date [19].

In this work, several mixtures of the solvents methanol, ethanol and isopropanol in water at different air/acetylene ratios were assayed. Their combined effect on Mg signal was evaluated by obtaining the surface responses. Calculations of the droplet sizes of the solvents mixtures and temperature estimations of the different zones of the perforated flame furnace were also performed as tools to explain their joint effect on the desolvation/atomization dynamics. Estimations of temperature were based on the two color thermometry method [20–23] which was modified by the authors for this particular purpose. The findings were employed to hypothesize about the sample behavior inside the furnace as it is explained throughout the manuscript.

Once obtained the operational variables giving the best performance, Mg was determined in Berocca(R) effervescent vitamin tablets. The samples were simply dissolved in either ethanol/water or methanol/water mixtures and then, directly introduced into the TS device. Validation was performed via FAAS after microwave digestion since it was not possible to prevent the nebulizer clogging by direct dissolution in alcohol/water. Results were in good agreement. Costs and economy of the analytical determination reveal that TS could be an excellent alternative not only for Mg but to other elements of lower volatility.

2. Experimental

2.1. Reagents and materials

All solutions were prepared with analytical grade chemical reagents and double deionised water (DIW) obtained from a Milli-Q purification system (Millipore, Bedford, MA, USA). All glassware was washed with EXTRAN (Merck, Darmstadt Germany) 1% v/v and kept in 10% (v/v) HCl (Merck) with further cleaning with DIW.

Mg standard solutions were prepared daily by appropriate dilutions of 1000 mg L^{-1} stock standard solution (Merck).

Organic solvents methanol, ethanol and isopropanol were Merck p.a.

Concentrated nitric acid was Merck p.a.

2.2. Instrumental

A flame atomic absorption spectrometer Shimadzu AAS 6800 (Kyoto, Japan) equipped with a hollow cathode lamp of Mg as radiation source and a deuterium lamp for background correction was used. Instrumental conditions were those provided by the manufacturer. An air/acetylene flame was used under different oxidant/fuel ratios: acetylene was varied between 1 and 3.5 L min^{-1} whilst air flow rate was kept constant at 24 L min^{-1} since no changes in air flow rate are allowed by the Shimadzu spectrometer. The optimal values of acetylene flow rate were 2.5 L min^{-1} and 3.0 L min^{-1} for ethanol and methanol, respectively. These values were employed throughout the experiments.

Transient signals were recorded in the peak height mode. Sharpness and tallness of the obtained signals made unnecessary the use of peak area mode.

A closed-vessel microwave oven (MDS-2000, CEM Corporation, USA), equipped with temperature and pressure probes, was used in the samples digestion procedure. The mineralization program was that provided by the manufacturer.

The TS-FF-AAS system was assembled with a peristaltic pump of eight channels and six rollers (IPC, Ismatec, Glattbrugg-Zürich, Switzerland), a six-ports rotatory valve VICI (Valco Instruments, Houston, TX, USA), 0.5 mm i.d. PTFE® tubings, a ceramic capillary (0.5 mm i.d., 6 cm length) and a perforated (six holes) nickel flame furnace atomizer placed on an air/acetylene flame with the assistance of a homemade steel holder (see Fig. 1).

The nickel tube (Inconel 600® alloy, Camacam, São Paulo, Brazil) composition was >72% (m/m) Ni, 14–17% (m/m) Cr and 6–10% Fe as major constituents. The dimensions were 9.7 mm i.d. and 100 mm length.

Temperature estimations were carried out with a Nikon D3100 digital camera. Digital photographs of the heated tube were obtained between 600 and 1000 °C at intervals of 50 °C. A muffle (Heraeus) was employed for changing the temperature of the tube for calibration purposes. "Color" measurements were performed at fixed sensitivity and exposure values, Shutter speed of 1/10 s and an aperture of 6.3 were considered optimal for the temperature range employed for calibration.

Image processing was performed with MATLAB 8.0

2.3. Procedure

2.3.1. Analytical methodology

Whole tablets of Berocca® (about 5 g weight) were microwave digested in nitric acid following the program provided by the

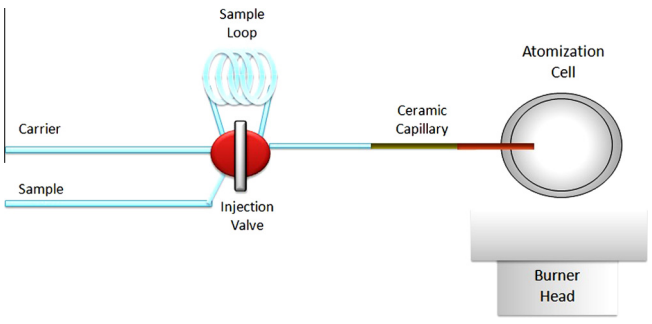

Fig. 1. TS-FFAAS experimental setup. Different proportions solvent/water were employed as carriers at a constant flow rate of 0.9 mL min^{-1}.

manufacturer (40 min length). The digested solution was made up to 100 mL with DIW and then, 30 μL were dissolved in 100 mL of DIW and analyzed by FAAS.

In the case of TS-FF-AAS determination with methanol, the whole tablet was dissolved in methanol/water 75% v/v and made up to 100 mL with the same solution, then 400 μL were dissolved in 100 mL of the same solvents mixture. The dissolved tablet was injected into the TS at a flow rate of 0.9 ml min^{-1} of the matching carrier. Acetylene flow rate was fixed at 3.0 L min^{-1}.As alternative, a TS-FFAAS determination of Mg in a dissolution of 75% v/v ethanol/water was assayed. Then, the procedure was followed as in the case of methanol except that acetylene flow rate was fixed at 2.5 L min^{-1}.

Spiking tests were performed by adding 200 μL of Mg standard solution 1000 mg L^{-1} to 400 μL of ethanol/water dissolution and then, made up to 100 mL with the same mixture.

2.3.2. Temperature distribution estimation

As described in the literature [19–23] and assuming that the metallic furnace behaves as a gray body, the temperature of the furnace is related to its light emission at two different wavelengths according to Eq. (1).

$$\frac{1}{T} = A^{*} ln\left(\frac{\lambda 1}{\lambda 2}\right) + B \quad (1)$$

where $\lambda 1$ and $\lambda 2$ are the signals obtained for two different channels (green and red or blue and green). A and B are constants that depend on the selected wavelength, the sensitivity of the camera at the different wavelengths and the emissivity of the material. Since the channels of the digital camera are not monochromatic as the optical filters can isolate a broad band of wavelengths, we needed to calibrate temperature. For doing this, the metallic furnace was placed inside a muffle and heated as described under Section 2.2. Then, photographs at the different temperatures were taken and the channels red, green and blue of the digital photograph were used as input data to solve Eq. (1).

Table 1 shows the correlation between the observed color in the original photograph and the estimated temperature values when the green/red and the blue/green channels are employed to solve Eq. (1). Mean temperature and error (in percentage) are also shown.

Table 1
Original pixels values of the heated furnace. Estimation of temperature through Green/Red and Blue/Green channels).

Temperature (°C)	R	G	B	Observed color	*T* estimation (°C) channels: G/R	*T* estimation (°C) channels: B/G	Mean temperature (°C)	% Error
600	23	2	6		606.33	590.46	598.40	0.27
650	89	11	20		648.84	653.04	650.94	−0.14
700	141	27	35		710.90	703.41	707.15	−1.02
750	176	43	42		750.87	751.92	751.39	−0.19
800	183	49	35		767.08	813.99	790.54	1.18
850	210	72	40		814.55	871.79	843.17	0.80
900	230	120	60		910.21	898.54	904.37	−0.49
950	255	165	70		968.53	943.68	956.11	−0.64
1000	255	205	80		1035.43	968.42	1001.93	−0.19

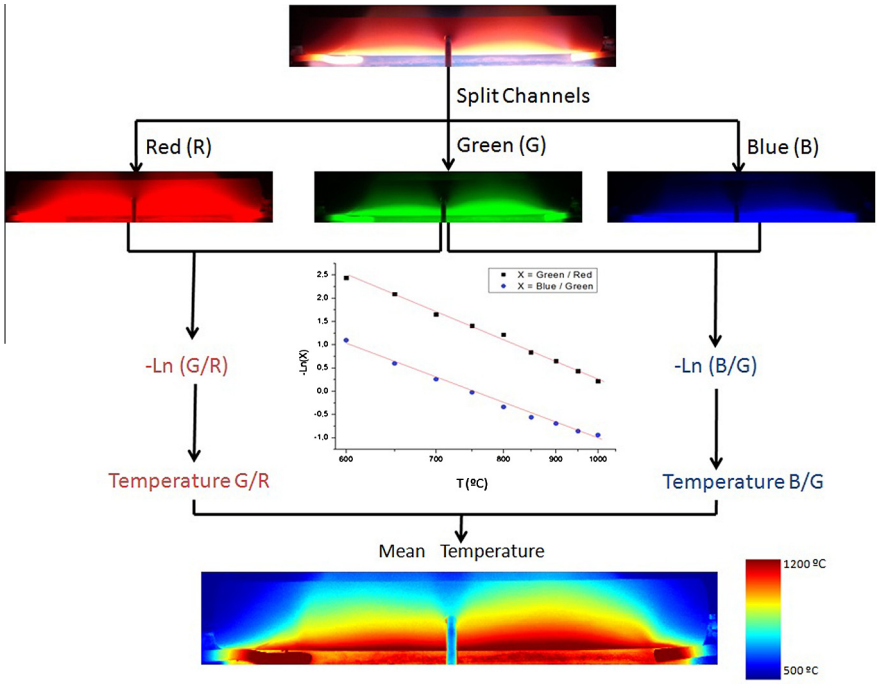

Fig. 2. Outline of the methodology used to estimate the temperature distribution. Calibration curve employed for temperature measurements.

Fig. 2 shows the linear relationship obtained by applying Eq. (1) for both, the green/red channel (G/R) and the blue/green channel (B/G), respectively.

3. Results and discussion

3.1. Influence of water soluble organic solvents on analytical signal

3.1.1. Organic solvents proportions and flame stoichiometry

To test the influence on the analytical signal of some water soluble organic solvents, mixtures of methanol, ethanol and i-propanol in DIW were prepared and evaluated as carriers. Mixtures ranged between 0 and 100% alcohol/water. 5 mg Mg L^{-1} solutions were prepared in each solvent mixture, and 500 μL of each solution were injected in a matching carrier at a fixed flow rate of 0.9 mL min^{-1}. Flame composition was varied between 1.0 and 3.5 L min^{-1} acetylene flow rate whilst air flow rate was kept constant. The signal of Mg in DIW was indistinguishable from the baseline noise. On the contrary, the addition of any of the solvents assayed increased the analytical signal.

A simple explanation could be that the mixture of the organic solvents with water in the samples and the matching carriers, reduces the amount of oxygen present in the atomization cell, generating a more suitable redox environment and probably preventing the formation of stable Mg oxygenated compounds. So, the addition of different proportions of organic compounds seemed to be capable of consuming oxygen by combustion. Further explanations will be provided below.

3.1.2. Droplet size

Another aspect to consider is the changes on the droplet size promoted by the presence of the different organic solvents. It has been demonstrated [24–26] that the average droplet size could be satisfactory predicted by Elkotb equation:

$$\mathrm{SMD} = 3.08 \cdot \nu_L^{0.385} \cdot \sigma_L^{0.737} \cdot \rho_L^{0.737} \cdot \rho_G^{0.06} \cdot \Delta p_L^{-0.54} \quad (2)$$

where ν_L is the liquid kinematic viscosity in Pa s^{-1}, σ_L is the liquid surface tension in mN m^{-1}, ρ_L and ρ_G are liquid and gaseous phase densities in kg m^{-3}, Δp_L is the pressure variation through the nozzle in Pa and SMD is the Sauter mean diameter in meters.

It is well known that water solutions of organic solvents have lower densities and surface tensions, therefore, the droplet size decreases as the organic proportion of the mixtures increases.

Fig. 3 shows the Sauter Mean Diameter for the different proportions of alcohol/water solutions as calculated through Eq. (2) [27–29]. It is observed that the average droplet size lowers as the alcohol proportion in water increases, which could render a faster desolvation/atomization kinetics and thus, an enhanced analytical signal.

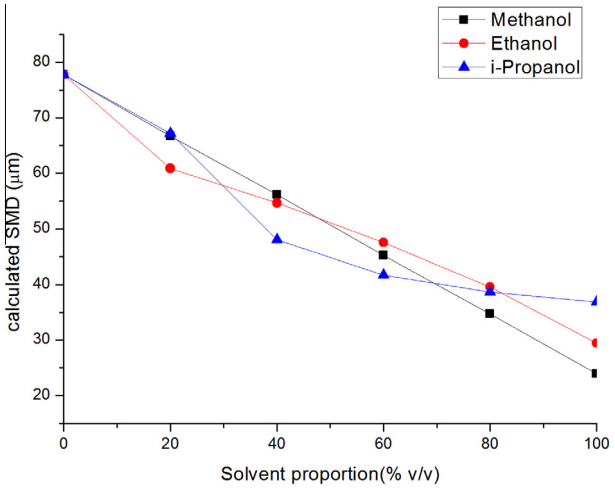

Fig. 3. Droplet size as a function of the organic solvent/water proportions used as carriers.

3.1.3. Combined effect organic solvents/flame stoichiometry

Since the presence of solvents influences the flame stoichiometry and thus its temperature, the most adequate proportion of solvent seems to be a compromise between the redox environment and the flame temperature.

Consequently, in order to study the joint effect of the alcohol/water proportions and the flame stoichiometry on the analytical signal of Mg, the experiments described under Section 3.1.1 were repeated at acetylene flow rates ranging between 1 and 3.5 L min^{-1} Air flow rate was kept constant at 24 L min^{-1}. Flow measurements indicated that 2 L min^{-1} acetylene flow rate is a stoichiometric flame, being fuel rich from this value onwards and fuel lean below this value. The results are shown in Fig. 4.

At a constant acetylene/air ratio, the first climb up of the signal whilst increasing the proportion of organics could be explained by the fact that the addition of organic solvents provides carbon atoms to the solution. This gives a more favorable reducing environment inside the tube, thus improving the atomization process.

Moreover, these solvents significantly lower the surface tension of the solution and its density being both directly related to droplet size of the primary aerosol and thus, to the analytical sensitivity.

On the other hand, at constant organic proportion, the first increment in the acetylene/air ratio reduces the oxygen present and favors the reducing environment, yielding an increment in the analytical sensitivity with no substantial change in the droplet size. Nonetheless and after reaching a maximum, the sensitivity drops again probably due to the cooling of the environment inside the atomization cell.

Then, the response surfaces shapes shown in Fig. 4 could be explained as a compromise between the droplet size of the primary aerosol, the reducing environment and the temperature of the atomization cell which is also decreased under reducing conditions.

Fig. 4 also shows that the position of the maximum and the peak height for the three alcohols are slightly different even though the droplet sizes are approximately the same at the same solvent proportion. In the case of methanol the maximum is found at 75% v/v and 3 L min^{-1} acetylene flow rate. However, in the case of ethanol, the maximum is lower than in the methanol case, and it is found at the same organic proportion but at a lower acetylene/air ratio. This is probably due to the number of carbon atoms in the molecule: ethanol consumes twice oxygen than methanol, producing a more reducing environment at lower organic proportion. Also, because of a major influence on the flame stoichiometry, it could be said that the temperature drops faster for ethanol. This could explain why the analytical signal for ethanol under optimized conditions is lower than the analytical signal for methanol. Following the same tendency, i-propanol not only has its maximum at a lower solvent proportion but also at a lower acetylene/air ratio. This could explain why its reducing capacity is higher than the others and why the stoichiometry of the flame is rapidly affected, rendering an optimum redox environment at smaller acetylene/air ratio in comparison to the others.

3.1.4. Temperature distribution of the atomization cell

Figs. 5 and 6 show an axial view of the distribution of temperature in the atomization cell under different operational conditions.

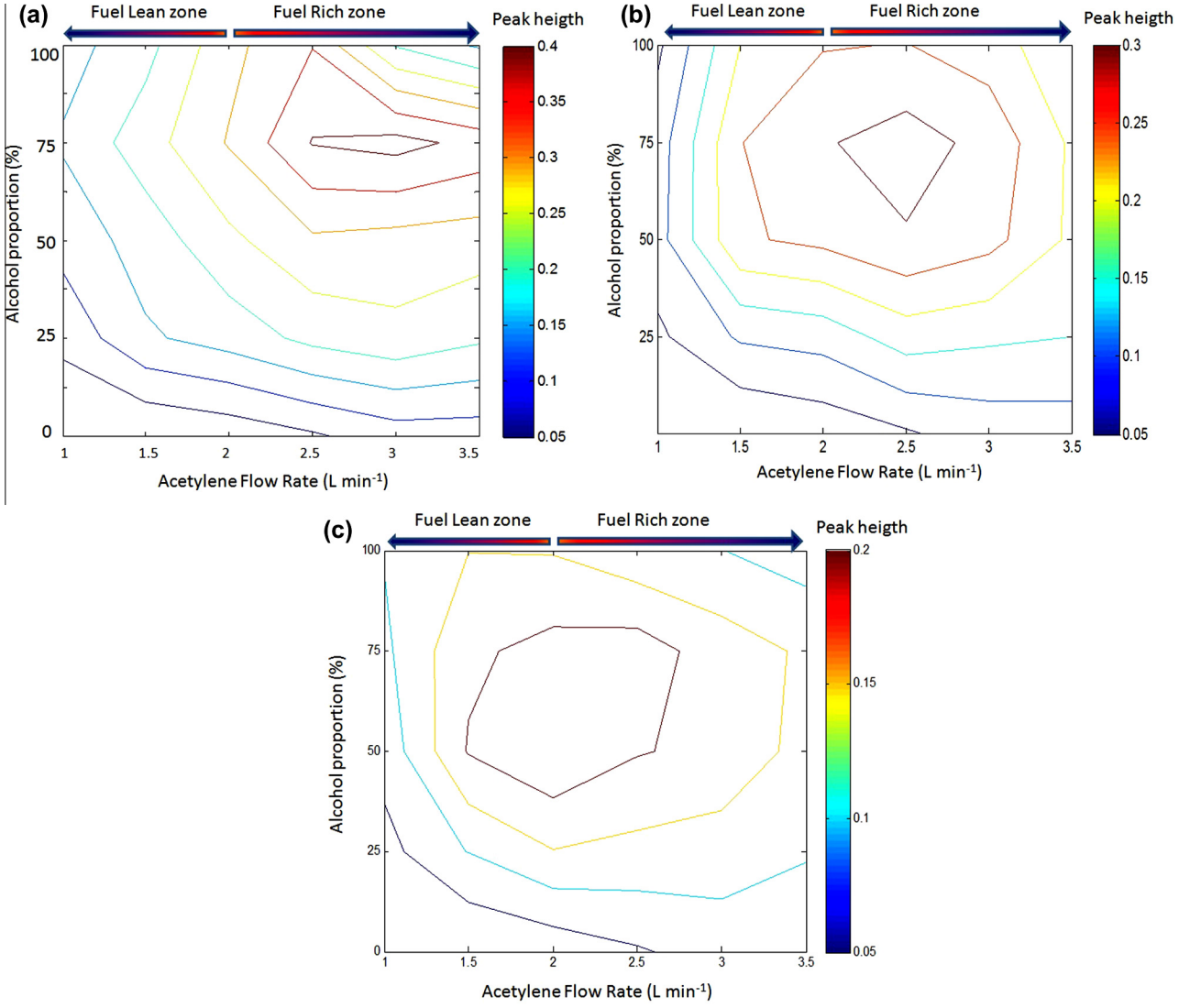

Fig. 4. Influence of alcohol/water proportions and flame stoichiometry on the analytical signal of Mg. Response surfaces for different alcohols solutions at different flame stoichiometric conditions: (a) methanol/water; (b) ethanol/water; (c) isopropanol/water.

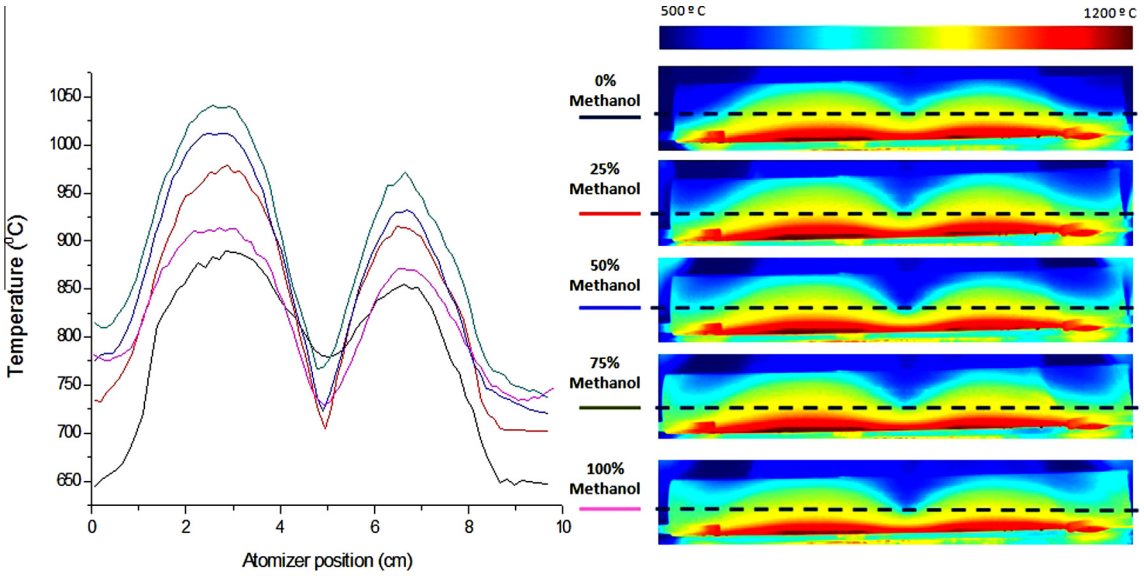

Fig. 5. Axial temperature distribution of the atomizer employing different methanol/water mixtures.

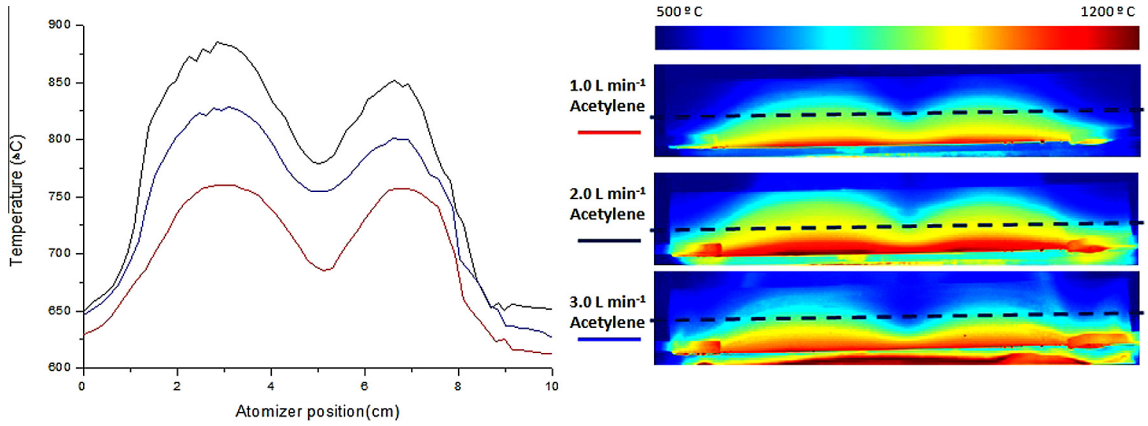

Fig. 6. Axial temperature distribution of the atomizer using different acetylene flow rates.

Correlation between temperature and "color" measurements in the original pictures (rear part) was performed as described under Section 2.3.2. As expected, it is observed a temperature decrease from the base of the tube – in direct contact with the flame – towards the top and along the atomizer. In all cases, it is also noticed an important temperature fall at the center of the tube. This is consistent with the impact site of the solvent jet in the center of the cell, which consumes energy from the tube wall for vaporizing the solvent. Consequently, the drop on temperature in the central zone makes inefficient the vapor production. Therefore, two different zones can be established: (a) the desolvation zone or central zone, where the energy is mainly employed to evaporate the solvent, to reduce the droplet size during the collision between the solvent jet and the heated wall, and to desolvate the analyte ions; and (b) the atomization zone, at both sides of the desolvation zone, where the energy is mostly employed for atomization.

Table 2
Comparison of figures of merit for the conventional analysis and the optimized TS-FFAAS conditions for methanol and ethanol, both 75% v/v.

	TS-FF-AAS (MeOH)	TS-FF-AAS (EtOH)
Sensitivity^{-1} (mg L^{-1})	0.086 ± 0.04	0.063 ± 0.05
Dynamic linear range (mg L^{-1})	0.068–5	0.09–5
%RSD (n = 5)	3.55%	4.02%
LOD (mg L^{-1}) (3 σb)	0.021	0.027
LOQ (mg L^{-1}) (10 σb)	0.068	0.090
Sample throughput (h^{-1})*	60	60

* Time for sample preparation was added to calculate sample throughput in all cases.

Fig. 5 shows the temperature distribution of the atomizer along the optical path, employing different methanol/water mixtures introduced into the perforated flame furnace at 0.9 mL min^{-1} and 2.0 L min^{-1} acetylene flow rate. The right side of the figure shows a color scale that can be correlated with temperature. The dotted line in the middle of the tube shows the position at which the temperature profile was captured and helps on understanding the comparison in the figure of the left.

It could be seen that the temperature in the center (desolvation zone) decreases if the carrier is enriched in the organic solvent. The temperature in the atomization zone increases with the methanol proportion up to 75% v/v and then, drops again. This tendency is consistent with the signal of Mg and agrees with the discussion presented above.

Fig. 6 illustrates the axial temperature distribution of the perforated atomizer using different acetylene flow rates. Carrier flow rate was kept equal to 0.9 mL min^{-1}. This figure shows the influence of the acetylene flow rate on the atomizer temperature. It can be noticed that the highest temperature is reached under stoichiometric conditions (2.0 L min^{-1}). Fuel leaner or fuel richer flames show lower temperatures in agreement with the basic literature on FAAS.

3.2. Analysis of vitamin tablet

Table 2 shows the figures of merit obtained for the TS determination with methanol/water and ethanol/water at the optimized conditions explained above. Table 4 shows the recovery results obtained by adding standard solutions of Mg to a

Table 3
Mg determination in Berocca effervescent tablet: FAAS with sample digestion; TS-FFAAS with direct introduction of sample for methanol and ethanol, under optimized conditions. (Results expressed as mean ± std. deviation).

Method	Sample 1 (mg Mg per tablet)	Sample 2 (mg Mg per tablet)	Sample 3 (mg Mg per tablet)	Sample 4 (mg Mg per tablet)	Sample 5 (mg Mg per tablet)
FAAS with simple digestion	102.3 ± 0.2	99.1 ± 0.2	98.2 ± 0.2	103.6 ± 0.2	97.8 ± 0.2
TS-FF-AAS (MeOH) without simple digestion	101.1 ± 0.2	98.9 ± 0.2	100.2 ± 0.2	104.5 ± 0.2	97.3 ± 0.2
TS-FF-AAS (EtOH) without simple digestion	90.8 ± 0.2	105.3 ± 0.2	98.4 ± 0.2	102.1 ± 0.2	99.6 ± 0.2

Table 4
Spiking experiments performed in five different samples of vitamin. Results expressed as recovery percent.

Method	Spiking sample 1 (% recovery)	Spiking sample 2 (% recovery)	Spiking sample 3 (% recovery)	Spiking sample 4 (% recovery)	Spiking sample 5 (% recovery)
TS-FF-AAS (MeOH)	101.4	100.4	98.2	99.3	100.7
TS-FF-AAS (EtOH)	98.6	99.6	101.8	100.7	99.3

suspension of Berocca vitamin tablets and measuring them by simple introduction into the TS device. The percentage of recovery for both solvents ranged between 98 and 101%. Although methanol shows a higher analytical sensitivity than ethanol, there is a slight difference and ethanol solutions were preferred due to its lower toxicity.

Table 3 shows the analytical results obtained by the methodology described here. A good agreement was found when compared to FAAS for a 95% confidence level (t student, $n = 5$) with the advantage that there is no need for sample mineralization by employing TS. Also, a reduction in the amount of reagents and waste is obtained with a considerable decrease of costs.

Moreover, since mineralization of samples is prone to contamination, the TS-FFAAS seems attractive as it allows a very simple pretreatment, direct injection into the equipment (slurry sampling) and external calibration for quantitation.

4. Conclusions

The main objective of this study is to show that a suitable management of the operational variables in TS-FF-AAS allows broadening its analytical capabilities.

This work shows for the first time that an analytical signal different from zero can be obtained for Mg via TS, that a direct introduction of the sample can be carried out with no need of samples digestion yielding a higher sample throughput and a sensitive reduction in reagents consumption and waste, and that the obtained results are in good agreement with FAAS methodology.

Conflict of interest

There is no conflict of interest.

Acknowledgments

To UBACyT (Science and Technology of Buenos Aires University) and CONICET (National Council of Science and Technology) for financial support.

MBT is researcher from CONICET and EMM is a doctoral fellow.

References

[1] A. Gáspár, H. Berndt, Thermospray flame furnace atomic absorption spectrometry (TS-FF-AAS)— a simple method for trace element determination with microsamples in the μg/l concentration range, Spectrochim. Acta Part B 55 (2000) 587–597.
[2] C.C. Nascentes, M.Y. Kamogawa, K.G. Fernandes, M.A.Z. Arruda, A.R.A. Nogueira, J.A. Nóbrega, Direct determination of Cu, Mn, Pb, and Zn in beer by thermospray flame furnace atomic absorption spectrometry, Spectrochim. Acta Part B 60 (2005) 749–753.
[3] C.R.T. Tarley, A.F. Barbosa, M.G. Segatelli, E.C. Figueiredo, P.O. Luccas, Highly improved sensitivity of TS-FF-AAS for Cd(II) determination at ng L-1 levels using a simple flow injection minicolumn preconcentration system with multiwall carbon nanotubes, J. Anal. At. Spectrom. 21 (2006) 1305–1313.
[4] M.L. Brancalion, M.A.Z. Arruda, Evaluation of medicinal plant decomposition efficiency using microwave ovens and mini-vials for Cd determination by TS-FF-AAS, Microchim. Acta 150 (2005) 283–290.
[5] M. da Silva Gomes, E. Rodrigues Pereira-Filho, Ti and Ni tubes combined in thermospray flame furnace atomic absorption spectrometry (TS-FF-AAS) for the determination of copper in biological samples, Microchem. J. 93 (2009) 93–98.
[6] G.L. Donati, C.C. Nascentes, A.R.A. Nogueira, M.A.Z. Arruda, J.A. Nobréga, Acid extraction and cloud point preconcentration as sample preparation strategies for cobalt determination in biological materials by thermospray flame furnace atomic absorption spectrometry, Microchem. J. 82 (2006) 189–195.
[7] E. Morzan, O. Piano, J. Stripeikis, M. Tudino, Evaluation of quartz tubes as atomization cells for gold determination by thermospray flame furnace atomic absorption spectrometry, Spectrochim. Acta Part B 77 (2012) 58–62.
[8] K. Miranda, A. G.G. Dionísio, O.D. Pessoa Neto, M.S. Gomes, E.R. Pereira-Filho, Determination of Cd levels in smoke condensate of Brazilian and Paraguayan cigarettes by Thermospray Flame Furnace Atomic Absorption Spectrometry (TS-FF-AAS), Microchem. J. 100 (2012) 27–30.
[9] F. Gerondi, M.A.Z. Arruda, Thermospray flame furnace atomic absorption spectrometry for determination of silver in biological materials, Talanta 97 (2012) 395–399.
[10] G.A. Petrucelli, R.J. Poppi, R.L. Mincato, E.R. Pereira, TS-FF-AAS and multivariate calibration: a proposition for sewage sludge slurry sample analyses, Talanta 71 (2007) 620–626.
[11] F. Rosini, C.C. Nascentes, J.Y. Neira, J.A. Nóbrega, Evaluation of selenium behavior in thermospray flame furnace atomic absorption spectrometry, Talanta 73 (2007) 845–849.
[12] H. Berndt, E. Pulvermacher, Sample introduction assisted by compressed air in flame furnace AAS: a simple and sensitive method for the determination of traces of toxic elements, Anal. Bioanal. Chem. 382 (2005) 1826–1834.
[13] G.D. Matos, M.A.Z. Arruda, Improvements in cobalt determination by thermospray flame furnace atomic absorption spectrometry using an on-line derivatization strategy, Talanta 76 (2008) 475–478.
[14] P. Wu, Y. Zhang, Y. Lv, X. Hou, Cloud point extraction–thermospray flame quartz furnace atomic absorption spectrometry for determination of ultratrace cadmium in water and urine, Spectrochim. Acta Part B 61 (2006) 1310–1314.
[15] P. Wu, Y. Zhang, R. Liu, Y. Lv, X. Hou, Comparison of tungsten coil electrothermal vaporization and thermospray sample introduction methods for flame furnace atomic absorption spectrometry, Talanta 77 (2009) 1778–1782.
[16] D.J. Liberato, A.L. Yergey, N. Esteban, C.E. Gomez-Sanchez, C.H.L. Shackleton, Thermospray HPLC/MS: a new mass spectrometric technique for the profiling of steroids, J. Steroid Biochem. 27 (1987) 61–70.
[17] S.L. Abidi, S.C. Ha, R.T. Rosen, Liquid chromatography—thermospray mass spectrometric study of N-acylamino dilactones and 4-butyrolactones derived from antimycin, J. Chromatogr. A 522 (1990) 179–194.
[18] M. Yamane, High-performance liquid chromatography–thermospray ionization-mass spectrometry of the oxidation products of polyunsaturated-fatty acids, Anal. Chim. Acta 465 (2002) 227–236.
[19] J. Mora, A. Canals, V. Hernandis, Behaviour of the thermospray nebulizer as a system for the introduction of organic solutions in flame atomic absorption spectrometry, Spectrochim. Acta Part B 51 (1996) 1535–1549.
[20] D. P. De Witt, G. D. Nutter; Theory and Practice of Radiation Thermometry; John Wiley & Sons Inc. 1989.
[21] Yan, J., Li, W., Research on colorimetric temperature-measurement method improved based on CCD imaging In: Proceedings – 2010 3rd International Congress on Image and Signal Processing, (2010), 189–192.
[22] Jiao Shuqing Design on the Real-time Measurement Method of Molten Metal HighTemperature Based on DSP, Ninth International Conference on Computational Intelligence and Security (2013), 533–536.
[23] Danping Jia, Jinhui Chen, Hongli San, Liang He On-line Temperature Measurement System for Carbonization Chamber Wall of Coke Oven, 2012 International Workshop on Information and Electronics Engineering (IWIEE), Procedia Engineering 29 (2012) 2869-2873
[24] M. Almeida Bezerra, V. Azevedo Lemos, J. Simone Garcia, D. Gonçalves da Silva, A. Souza Araújo, M. A. Z. Arruda, Thermospray generation directly into a flame furnaceAn alternative to improve the detection power in atomic absorption spectrometry, Talanta 82 (2010) 437–443.
[25] M.L. Brancalion, E. Sabadini, M.A.Z. Arruda, Thermospray nebulization for flame furnace atomic absorption spectrometry—Correlations between spray formation and cadmium analytical sensitivity, Spectrochim. Acta Part B 64 (2009) 89–94.
[26] M.L. Brancalion, E. Sabadini, M.A.Z. Arruda, Description of the thermospray formed at low flow rate in thermospray flame furnace atomic absorption spectrometry based on high-speed images, Anal. Chem. 79 (2007) 6527–6533.
[27] F. Pang, C. Seng, T. Teng, M.H. Ibrahim, Densities and viscosities of aqueous solutions of 1-propanol and 2-propanol at temperatures from 293.15 K to 333.15 K, J. Mol. Liq. 136 (2007) 71–78.
[28] D.R. Lide (Ed.), Handbook of Chemistry and Physics: A Ready Reference Book of Chemical and Physical Data, 82nd ed., CRC Press, Chemical Rubber, Boca Raton (FL), 2001–2002.
[29] A. Nikumbh, G. Kulkarni, Density and viscosity study of binary mixtures of ethanol – water at different temperatures science, J. Pure Appl. Chem. 196 (2013) 1–13.